JOURNAL OF GEOPHYSICAL RESEARCH, VOL. 102, NO. A5, PAGES 9619-9629, MAY 1, 1997

# A statistical study of giant pulsation latitudinal polarization and amplitude variation

G. Chisham and I. R. Mann

Astronomy Unit, Queen Mary and Westfield College, London

D. Orr

Department of Physics, University of York, York

**Abstract.** Using data from 34 Pg events observed by the European incoherent scatter (EISCAT) magnetometer cross, we complete a statistical study of the horizontal polarization and amplitude variation of Pgs with latitude. The polarization statistics consistently display the same latitudinal variation, being exclusively anticlockwise equatorward of linear polarization and exclusively clockwise poleward of linear polarization. The polarization azimuth (or ellipse orientation) changes from an approximately northeast to southwest orientation equatorward of linear polarization to an approximately northwest to southeast orientation poleward of linear polarization. However, the oscillations are not polarized exactly east-west at linear polarization but some distance poleward of linear polarization. The amplitude statistics for the $D$ component display the distinct latitudinal variation characteristic of a resonance, whilst the $H$ component is less well defined and has a tendency to dip at the position of the $D$ component maximum. We employ an MHD model to describe the evolution of Pg-like waves and compare the numerical results to the observational statistics. We suggest that a mechanism such as drift bounce resonance drives a radially (poloidally) polarized wave of limited radial width on $L$ shells where the instability is operative. This mechanism favors large azimuthal wave numbers and drives dominantly Alfvénic waves. Because of their incompressible nature, these waves also possess an azimuthal (toroidal) component with a radial amplitude variation proportional to the radial gradient of the poloidal component. Hence the toroidal amplitude variation will be double peaked with a node at the position of the poloidal peak. This is in good agreement with the ground-based observations as the toroidal (poloidal) oscillations map to $H$ ($D$) component oscillations on the ground due to the 90° rotation of Alfvén waves by the ionosphere. Once driven these waves evolve due to the presence of the radial plasma inhomogeneity, which causes the wave polarization to rotate from a poloidal to a toroidal configuration in time. We show how this can explain why the position of the east-west oriented polarization ellipse lies poleward of linear polarization. We conclude that Pgs are likely to be guided poloidal Alfvén waves which are being continually driven by a population of westward drifting energetic protons and also speculate about the evolution of poloidal Alfvén waves in the afternoon sector of the magnetosphere.

## 1. Introduction

Giant pulsations (Pgs) are probably the most intriging of all magnetospheric ULF wave phenomena that have been observed by ground-based instrumentation. Pgs are ULF waves in the Pc 4 period range (45-150 s) and are characterized by their sinusoidal appearance and long duration of wavepacket. They occur in the early morning hours, predominantly around the equinoxes in years of solar minimum [*Brekke et al.*, 1987]. Pgs are almost exclusively auroral zone phenomena, occur most often just poleward of the equatorward edge of the auroral oval [*Chisham and Orr*, 1994] and are characterized by a localization in latitude [*Glassmeier*, 1980; *Chisham et al.*, 1990] and moderately large azimuthal wave numbers [e.g., *Chisham et al.*, 1992].

Pgs have been well defined over the last 20 years with observations from magnetometer chains [*Green*,



Paper number 97JA00325.
0148-0227/97/97JA-00325$09.00

1979, 1985; *Rostoker et al.*, 1979; *Chisham et al.*, 1990; *Chisham and Orr*, 1991], magnetometer arrays [*Glassmeier*, 1980; *Chisham et al.*, 1992; *Takahashi et al.*, 1992], spacecraft [*Hillebrand et al.*, 1982; *Kokubun et al.*, 1989; *Takahashi et al.*, 1992] and auroral radar [*Poulter et al.*, 1983; *Chisham et al.*, 1992]. They have also been observed in connection with pulsating auroral phenomena [*Taylor et al.*, 1989; *Chisham et al.*, 1990]. To date, however, there is still no universally accepted generation mechanism, although it is generally agreed that Pgs are the result of a plasma instability that occurs inside the magnetosphere rather than a consequence of solar wind fluctuations as is thought to be the case with other Pc 4 pulsations [e.g., *Cao et al.*, 1994]. A possible generation mechanism for Pgs is the drift bounce resonance instability [*Southwood et al.*, 1969; *Southwood*, 1976] which would require the wave to be an even mode standing wave (e.g., a second harmonic). Resonantly generated waves should have large azimuthal wave numbers and be dominantly radially polarized [*Southwood*, 1976, 1980]. This instability has been suggested many times as a possible Pg excitation mechanism [e.g., *Glassmeier*, 1980; *Poulter et al.*, 1983; *Chisham et al.*, 1992].

One feature that distinguishes Pgs from other Pc 4 pulsations is their polarization. The magnetic field perturbations of the more frequently observed Pc 4 pulsations are generally dominated on the ground by the $H$ (geomagnetic north-south) component. This is in contrast to Pgs, which are generally dominated by the $D$ (geomagnetic east-west) component. This suggests that Pgs are predominantly radially polarized in the magnetosphere, if the waves are mainly of an Alfvénic nature (as suggested by *Chisham et al.* [1992]), due to the 90° rotation of Alfvén waves by the ionosphere [e.g., *Hughes and Southwood*, 1976]. Studying the horizontal polarization of ULF waves observed on the ground can provide important pointers toward unravelling the ULF wave structure in the magnetosphere.

The horizontal polarization of a ULF wave on the ground is described by two parameters, the ellipticity and azimuth (or ellipse orientation). The ellipticity variation of Pgs with latitude was studied statistically by *Hillebrand* [1976]. They showed that Pg polarization is clockwise poleward of a region of linear polarization and anticlockwise equatorward of this region (when viewed in the direction of the geomagnetic field line). These polarization variations have been confirmed by later observational work [*Glassmeier*, 1980; *Hillebrand et al.*, 1982; *Chisham et al.*, 1990]. The azimuth of the Pg polarization ellipse has received little attention in previous work. Most studies have merely commented that Pg polarization ellipses are predominantly oriented in the east-west direction on the ground. *Glassmeier* [1980] studied the polarization azimuths for one Pg event observed over a large magnetometer array. His results suggested that not only does the sense of polarization reverse at a particular latitude but that the polarization azimuths point toward a central region, thus defining a meridional separator line. However, this interpretation was made using results from only one event. No statistical study of Pg polarization azimuths has been previously undertaken. Likewise, no statistical study of the variation of the $H$ and $D$ component amplitudes with latitude has been undertaken. All previous theories have developed from looking at the amplitude and polarization profiles of a handful of events.

Thirty-four Pg events were observed by the European incoherent scatter (EISCAT) magnetometer cross in the period 1984 - 1987. We analyzed the amplitude and polarization characteristics of each of these 34 Pg events using the method of complex demodulation. These characteristics were averaged over the central 50% of each event (where the values are relatively stable; see *Chisham and Orr* [1991]) to provide average amplitude and polarization estimates at each station for each event. In this paper, we present the results of a statistical analysis of the polarization and amplitude characteristics of Pgs and subsequently employ an MHD model in an attempt to explain the typical features observed.

The paper is structured as follows: section 2 describes the data analysis techniques, while sections 3 and 4 outline the resulting polarization and amplitude statistics. In section 5 we model a Pg-like wave, and in section 6 we discuss a comparison between the model and the observed data. Section 7 summarizes and concludes the paper.

## 2. Data Analysis

The EISCAT magnetometer cross [*Lühr et al.*, 1984] is situated in northern Scandinavia and comprises an array of seven three-component fluxgate magnetometers with a sampling period of 20 s. Each instrument measures magnetic field variations over a range of ±2000 nT with a resolution of 1 nT. The EISCAT magnetometer cross data were rotated from geographic to geomagnetic coordinates ($X$,$Y$,$Z$ to $H$,$D$,$Z$) for our analysis. In this study we only used data from the latitudinal chain of the EISCAT magnetometer cross so as to avoid misinterpreting any effects due to longitudinal phase changes. The geographic and corrected geomagetic coordinates of the stations we used are displayed in Table 1 along with the associated dipole field $L$ shell positions.

All the amplitude and polarization estimates in this study were made using the technique of complex demodulation [*Beamish et al.*, 1979]. This is a method of analysing particular frequency components of a waveform in terms of amplitude, phase, and polarization characteristics, and is based upon the fast Fourier transform (FFT). The polarization of a ULF wave can be described by two parameters, the ellipticity and the azimuth (or ellipse orientation). The ellipticity is given by the ratio of the minor axis to the major axis of the polarization ellipse; a negative ellipticity represents an

**Table 1.** Coordinates and $L$ Shell Values of the Latitudinal EISCAT Magnetometer Cross Stations

| Station | Code | Geographic Latitude | Geographic Longitude | Geomagnetic Latitude | Geomagnetic Longitude | $L$ Shell |
|---|---|---|---|---|---|---|
| Soroya | SOR | 70.54 | 22.22 | 67.01 | 106.91 | 6.66 |
| Alta | ALT | 69.86 | 22.96 | 66.28 | 106.83 | 6.28 |
| Kautokeino | KAU | 69.02 | 23.05 | 65.43 | 106.17 | 5.88 |
| Muonio | MUO | 68.01 | 23.53 | 64.39 | 105.73 | 5.44 |
| Pello | PEL | 66.90 | 24.08 | 63.23 | 105.34 | 5.01 |

All values were calculated using the IGRF for 1987 at an altitude of 120 km.

anticlockwise polarization and a positive ellipticity represents a clockwise polarization (as viewed in the direction of the geomagnetic field line). The polarization azimuth is 0° for a north-south orientation and increases positively as the polarization orientation rotates clockwise, being 90° for an east-west orientation and finally 180° for a north-south orientation.

Figure 1 displays a typical Pg event observed by the EISCAT magnetometer cross on December 29 1987 [*Chisham et al.*, 1992]. The wave signal is extremely sinusoidal and dominated by the $D$ component. The polarization variation associated with this event is presented in Figure 2. The ellipticity and azimuth variations displayed by this event are typical of the 34 Pgs.

## 3. Polarization Statistics

We studied the latitudinal variation of the polarization azimuth and ellipticity of the 34 Pg events by plotting the polarization estimates with respect to their distance from the region of linear polarization (an estimate of the resonant field line position). The $L$ shell of linear polarization was calculated for each event by interpolating between the ellipticities measured either side of the polarization reversal which is a characteristic of Pg events (see Figure 2).

Figure 3 displays the variation in Pg polarization ellipticity with $L$ shell distance from linear polarization. In this and the following figures, negative values refer to

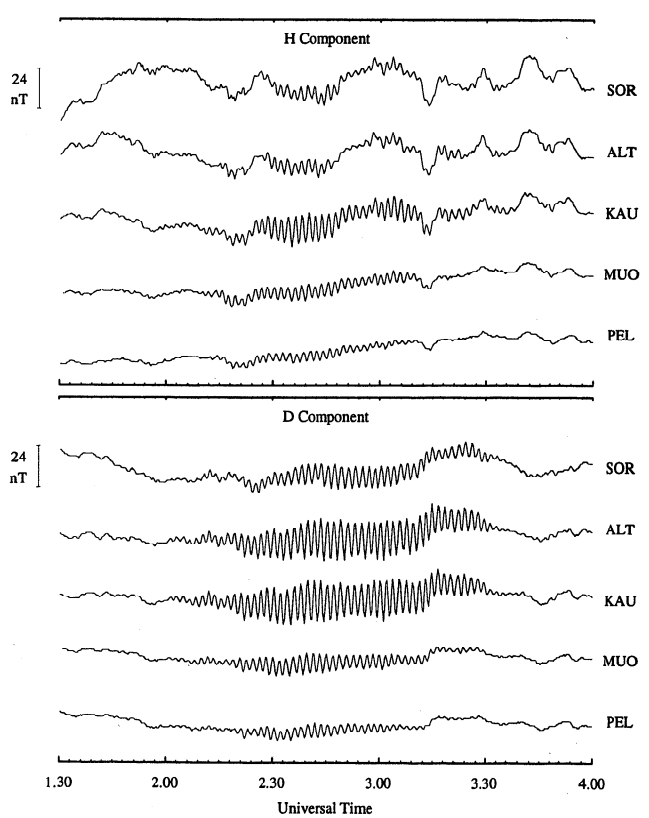


**Figure 1.** Unfiltered magnetograms displaying the $H$ (geomagnetic north-south) and $D$ (geomagnetic east-west) components of a Pg event observed by the latitudinal chain of the EISCAT magnetometer cross on 29 December 1987.

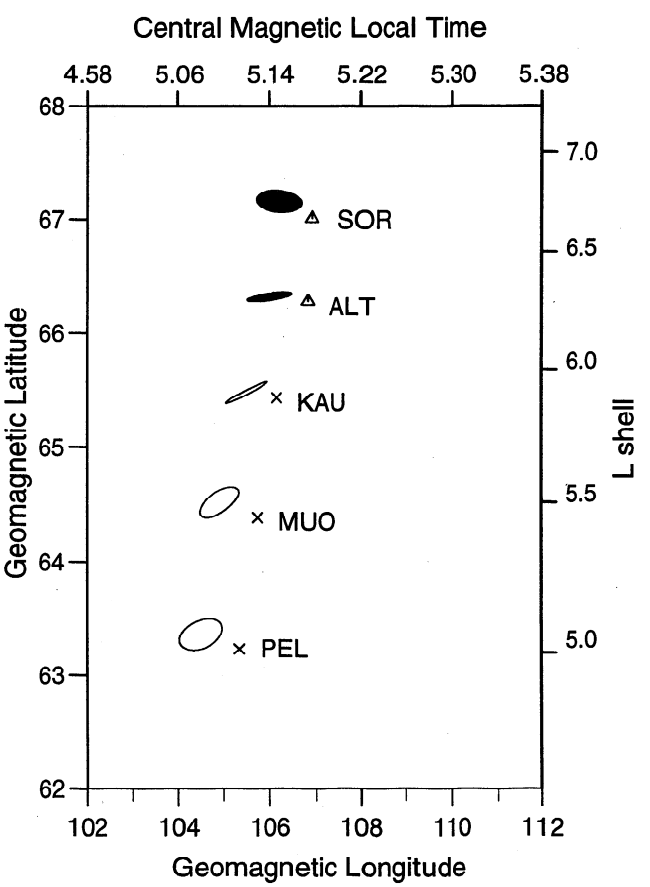


**Figure 2.** Latitudinal polarization variation of the Pg event displayed in Figure 1. The filled ellipses represent clockwise polarization, the unfilled ellipses represent anticlockwise polarization.

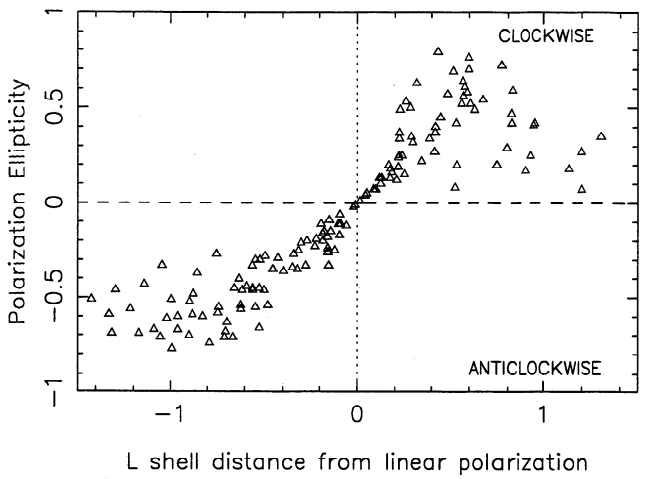


**Figure 3.** The statistical distribution of the measured polarization ellipticity of the 34 Pg events as a function of the distance of the measurement from linear polarization.

the $L$ shell distance equatorward of linear polarization and positive values refer to the $L$ shell distance poleward of linear polarization (hence the ellipticity distribution will cross zero at linear polarization). Figure 3 shows clearly that the polarization equatorward of linear polarization is exclusively anticlockwise whilst that poleward of linear polarization is exclusively clockwise. The polarization estimates become increasingly scattered more than 0.5 L away from linear polarization and this is probably a result of the low wave amplitudes at these points which would make these estimates unreliable.

Figure 4 displays the variation in Pg polarization azimuth with $L$ shell distance from linear polarization. At distances greater than 0.5 $L$ away from resonance, in both the poleward and equatorward directions, the azimuths are randomly spread from 0° to 180°. Again, this can be explained by the reduced signal-to-noise ratio making these values less reliable. Between -0.5 $L$ and 0.5 $L$ the majority of the azimuths are contained within a band approximately 45° wide that appears to change position while moving through the resonance position. Equatorward of the resonance position most of the azimuths are located between 45° and 90°. Poleward of the resonance position this band is located approximately between 60° and 105°. This represents a small but significant change in the polarization azimuth across resonance.

Figure 5 displays an alternative way of studying the variation in the polarization orientation across the resonance region. The region between -1.0 $L$ and 1.0 $L$ has been divided into 10 equal sections of size 0.2 $L$. In each of these sections the polarization azimuth estimates have been binned into 30° azimuth bins. The result of this binning is displayed as a series of histograms in Figure 5. The histograms show that equatorward of linear polarization the azimuths are split between the 30° - 60° and 60° - 90° ranges; at linear polarization the azimuths are predominantly in the 60° - 90° range; and poleward of linear polarization the azimuths are split predominantly between the 60° - 90° and 90° - 120° ranges. Figure 5 also shows the variation of the polarization azimuths averaged across the 0.2 $L$ shell bins. The triangular symbols represent these averaged values and the dashed line displays the variation across the resonance region. The average azimuth equatorward of the resonance region is $\sim 60°$. This value increases with increasing latitude (increasing $L$ shell), being $\sim 75°$ at linear polarization and $\sim 90°$ poleward of this.

The polarization statistics displayed in Figures 3, 4, and 5 indicate that one particular latitudinal polarization variation is predominant for Pg events. The polarization variation presented in Figure 2 is typical of this variation. The main features of the azimuth variation are that there is only a gradual change in the orientation across the array from approximately northwest to southeast poleward of resonance to approximately northeast to southwest equatorward of resonance. However, the polarization orientation is not exactly east-west at the position of linear polarization but some distance poleward of it.

The Pg polarization statistics have been studied without considering any effect that nonuniform ionospheric conductivities may have on the wave polarization rotation in the ionosphere [e.g., *Glassmeier*, 1984]. It has been shown [*Chisham et al.*, 1995] that the rotation of wave polarization in the ionosphere can be substantially altered from 90° due to the ionospheric conductivity gradients found at dawn. It is likely that gradients in ionospheric conductivity occur in the auroral zone, especially close to auroral arcs. However, during the quiet periods in which Pgs occur the Pg maxima are found well equatorward of the estimated positions of auroral arcs, so it is unlikely that the observed polarizations have been affected by these gradients except possibly well poleward of linear polarization.

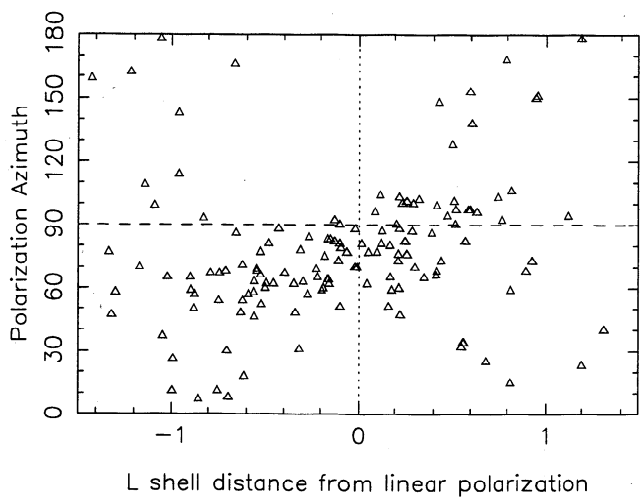


**Figure 4.** The statistical distribution of the measured polarization azimuth of the 34 Pg events as a function of the distance of the measurement from linear polarization.

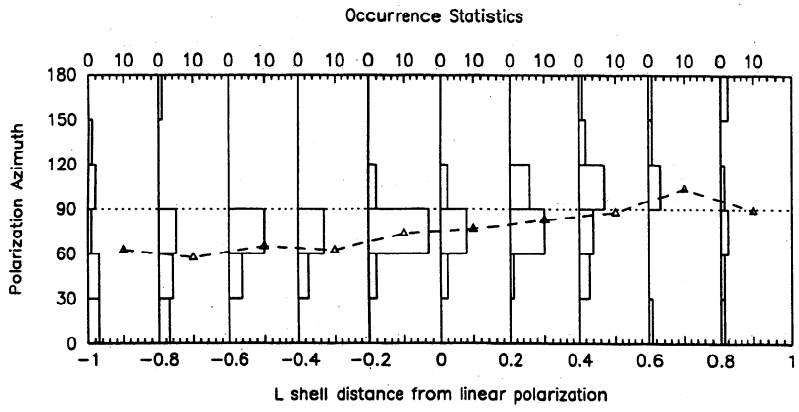


**Figure 5.** Histograms displaying the polarization azimuth variation either side of linear polarization. The polarization azimuths have been binned into 30° azimuth and 0.2 $L$ shell bins. The dashed line linking the triangular symbols represents the variation of the average value of the polarization azimuths calculated over each 0.2 $L$ shell bin.

## 4. Amplitude Statistics

We studied the latitudinal amplitude variations of the 34 Pg events by plotting the $H$ and $D$ components measured at each station as a fraction of the maximum $D$ component amplitude for that event against the $L$ shell distance from the $D$ component peak. The magnitude and $L$ shell position of the $D$ component peak were calculated by fitting a Gaussian curve to the latitudinal $D$ component amplitude variation. An example of this fitting is shown in Figure 6. The triangles represent the $D$ component amplitude profile, the filled squares represent the $H$ component amplitude profile and the solid line represents the gaussian fit to the $D$ component amplitude profile. Figure 6 shows that a Gaussian curve fits very well to the latitudinal $D$ component amplitude profile. This is the case for all of the 34 events.

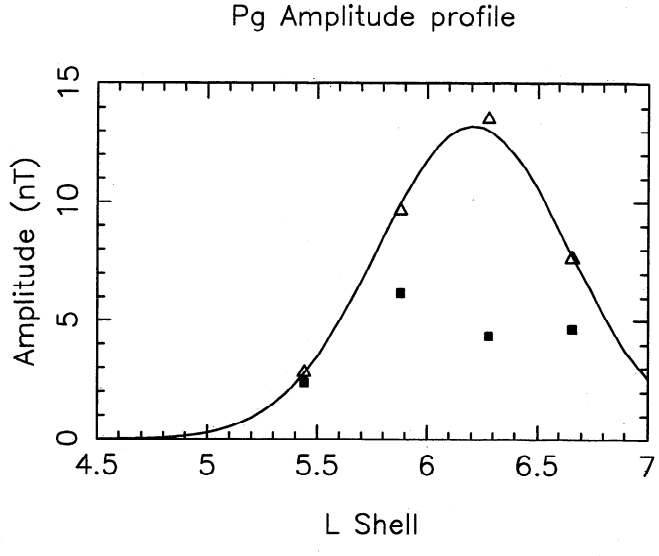


**Figure 6.** Gaussian fit (solid line) to the latitudinal $D$ component variation (triangles). Also shown is the latitudinal $H$ component variation (squares).

The figure also shows that the $H$ component amplitude is small compared to the $D$ component and suggests that a dip in the $H$ component amplitude occurs at the same position as the maximum $D$ component amplitude. Dips of this sort in the $H$ component amplitude profiles occur for 21 of the 34 Pg events. The other events either show a constant $H$ component amplitude profile with latitude or a peak that coincides with the $D$ component amplitude peak. Previous observations of Pgs [*Glassmeier*, 1980; *Takahashi et al.*, 1992] have displayed this $H$ component amplitude dip at the $D$ component maximum, but its occurrence has not been previously noted.

Figure 7 presents the statistical distribution of the $H$ and $D$ component amplitudes estimated from the 34 Pg events. The $D$ component amplitude variation (Figure 7a) is typical of that associated with a resonance. Figure 7a also shows that the latitudinal spatial extent of all the Pg events observed on the ground is almost exactly the same, being the equivalent of 2 Earth radii ($R_E$) in the magnetospheric equatorial plane. However, it is well known that due to the spatial integration of wave signals by the ionosphere the wave signal observed on the ground has a different spatial scale than that observed in the magnetosphere [*Poulter and Allan*, 1985]. It is likely that the latitudinal spatial extent of the pulsation observed on the ground is approximately twice that expected above the ionosphere. A good estimate of the radial extent of the wave disturbance in the magnetosphere is therefore $\sim 1\ R_E$.

Figure 7b displays the $H$ component amplitude distribution. It is clear that the striking peak which occurs in the $D$ component amplitude distribution is not present in the $H$ component distribution. In actuality, apart from a few points where an $H$ component amplitude maximum coincides with the $D$ component maximum, the general trend is for a slight dip to occur in the $H$ component amplitude profile. We consider the possible reasons for this by modelling a Pg-like wave in the following section.

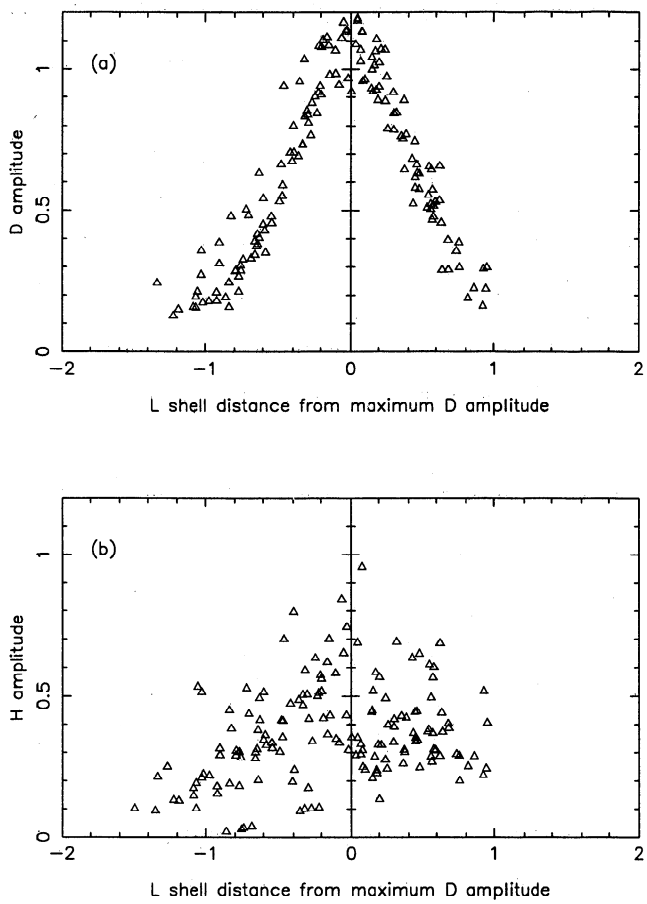


**Figure 7.** (a) The distribution of the measured $D$ component amplitudes. (b) The distribution of the measured $H$ component amplitudes.

## 5. Modeling of Pg Wave Events

In this section we solve for the evolution of Pg-like MHD waves and compare the results to both the Pg amplitude and polarization statistics. For simplicity, we consider the wave characteristics in a Cartesian box model magnetosphere [e.g., *Southwood*, 1974]. In this model the magnetic field is straightened out, uniform, and lies purely in the $\hat{\mathbf{z}}$ direction; i.e., $\mathbf{B} = B_0\hat{\mathbf{z}}$. We assume that the ionosphere is perfectly reflecting and that the waves are periodic in $\hat{\mathbf{y}}$ (analogous to the azimuthal direction in a dipole). The $\hat{\mathbf{x}}$ direction completes the triad and represents the radial (or $L$ shell) direction. We assume that the plasma is cold and solve for the $x$ and $t$ dependence of the plasma displacements by assuming variations of the form

$$\xi = (\xi_x(x,t), \xi_y(x,t), 0)e^{i\lambda y} \sin k_z z \tag{1}$$

where $\lambda$ and $k_z$ are the "azimuthal" and field-aligned wave numbers, respectively. We have normalized lengths with respect to the depth of the box (taken as $L_x = 5R_E$), magnetic fields by the ambient (uniform) magnetic field strength ($B_0$), and densities by the density in the center of the simulation $\hat{\mathbf{x}}$ domain. Consequently, time is normalized with respect to the Alfvén time given by $L_x/V_N$, where $V_N$ is the normalizing Alfvén speed ($V_N = \sqrt{B_0^2/\mu_0\rho_0}$).

By linearizing the ideal MHD equations [e.g., *Boyd and Sanderson*, 1969], magnetospheric waves in the box model can be described by the following normalized coupled differential equations [e.g., *Mann and Wright*, 1995]:

$$\frac{1}{v_A^2(x)}\frac{\partial^2\xi_x}{\partial t^2} + k_z^2\xi_x = -\frac{\partial b_z}{\partial x} \tag{2}$$

$$\frac{1}{v_A^2(x)}\frac{\partial^2\xi_y}{\partial t^2} + k_z^2\xi_y = -i\lambda b_z. \tag{3}$$

$$b_z = -\left(\frac{\partial\xi_x}{\partial x} + i\lambda\xi_y\right). \tag{4}$$

When $\lambda \to \infty$, $\xi_y \to 0$ and the poloidal ($\xi_x$) and toroidal ($\xi_y$) components of the waves decouple [*Dungey*, 1967; *Radoski*, 1967]. Equation (2) then describes poloidally polarized Alfvén waves, since when $\lambda$ is large, $b_z \sim \xi_y/\lambda \sim \xi_x/\lambda^2$, and to leading order (4) is the balance of [*Mann and Wright*, 1995]

$$\partial\xi_x/\partial x \sim -i\lambda\xi_y. \tag{5}$$

These waves propagate along the background magnetic field and constitute guided poloidal Alfvén waves having the general solution

$$\xi_x(x,t) = \xi_x(x,t=0)e^{i\omega_A(x)t} \tag{6}$$

where $\omega_A(x)$ is the local natural Alfvén frequency and $\xi_x(x,t=0)$ is the spatial envelope of the poloidal oscillations.

We assume that the waves in our simulation have been driven so that the initial $\xi_x$ and $\xi_y$ wave components oscillate in phase. In accordance with observations we assume that the initial poloidal wave disturbance is radially localized and has a Gaussian envelope of width $x_w$ given by

$$\xi_x(x,t=0) = \xi_{x0}e^{-(x-x_0)^2/x_w^2}, \tag{7}$$

and from (5), that the initial toroidal disturbance has an envelope of the form

$$\xi_y(x,t=0) = -\frac{2i}{\lambda}\frac{(x-x_0)}{x_w^2}\xi_x(x,t=0). \tag{8}$$

The initial physical magnetospheric plasma displacements are given by $\xi_x^P = \mathrm{Re}(\xi_x)$ and $\xi_y^P = \mathrm{Re}(\xi_y)$. We start the simualtions with the plasma at rest, and consequently both displacements initially oscillate as $\cos\omega_A(x)t$ and represent poloidal Alfvén waves which are standing in azimuth (as well as along the background magnetic field). Note that in the magnetosphere poloidal Alfvén waves are observed to have azimuthal phase propagation, perhaps as a result of being driven by the drift bounce resonance mechanism. Azimuthally propagating solutions may be synthesized by summing

two azimuthally standing solutions, one of which is presented here.

In a plasma with a radial inhomogeneity, the initial wave fields are expected to phase mix in time as each field line oscillates at its local Alfvén frequency. Adjacent field lines, initially in phase, gradually drift out of phase with each other in time, generating increasing radial gradients in the wave field [*Mann et al.*, 1995]. When $\lambda$ is large and finite, the poloidal wave amplitudes decay in time as they drive an additional toroidal response [*Mann and Wright*, 1995]. The toroidal amplitude grows to equal the (decayed) poloidal one on the timescale

$$\tau = \frac{\lambda}{\omega_A'}, \tag{9}$$

where $\omega_A' = d\omega_A/dx$, and where $\tau$ is the time taken for the radial length scales to phase mix down to the azimuthal scale $2\pi/\lambda$. The additional physical displacement $\xi_y^P$, which develops due to the wave evolution, is again given by (5), but oscillates as $\sin\omega_A(x)t$. Its leading order growth is determined by the phase mixing gradients developed in time by the $\exp(-i\omega_A(x)t)$ part of the poloidal Alfvén wave solution, and consequently we expect [*Mann and Wright*, 1995]

$$\xi_y^P \approx \frac{\omega_A'(x)t}{\lambda} \sin\lambda y \sin\omega_A(x)t\, \xi_{x0} e^{-(x-x_0)^2/x_w^2}. \tag{10}$$

Using the numerical code described by *Mann and Wright* [1995], we solve for the time dependent wave solutions. The initial disturbance is a standing second harmonic poloidal Alfvén wave whose amplitudes are Fourier approximations to the functions given in (7) and (8). (Note any harmonic could be modelled in this way.) We choose $\lambda = 23$ (to approximate a magnetospheric Pg with azimuthal wave number $m = 30$ at $L = 6.5$), $x_w = 0.1$ (i.e., $0.5R_E$), and $k_z = 1.93$ (assuming a field line length of $2.5L$). The local Alfvén frequency gradient is defined by the Alfvén speed variation (since $k_z$ is a constant), and we assume a monotonic variation of the form

$$v_A^{-2}(x) = A^2 - B^2\cos(\pi x) \tag{11}$$

where $A^2 = 1.0$ and $B^2 = 0.2$. The energy densities associated with the guided poloidal ($e_p$) and the toroidal ($e_t$) oscillations are defined as by *Mann and Wright* [1995]. The compressional energy density $e_c$ is initially zero and remains small compared to $e_p$ and $e_t$ throughout our simulation. The initial $e_p$ and $e_t$ energy density envelopes are plotted as solid lines in Figures 8a and 8b. Using the ordering in (5) and differentiating the initial Gaussian poloidal amplitude envelope with respect to $x$ predicts a latitudinally double-peaked amplitude envelope for the toroidal component which is in good agreement with the ground based magnetometer observations. In a nonuniform magnetosphere, these envelopes will evolve in time and it is important to analyse this behaviour.

The series of dashed lines in Figures 8a and 8b show the radial variation of the poloidal and toroidal energy densities respectively, at times in multiples of $0.5\tau$. Figures 8a and 8b illustrate how undriven, undamped poloidal Alfvén waves evolve towards an asymptotic toroidal polarization (as first shown by *Mann and Wright* [1995]). Moreover, the initial double-peaked toroidal variation becomes increasingly less well defined, until after a time $\gtrsim \tau$ the double peak is no longer apparent and the toroidal variation evolves toward a single peak centered on the resonant field line. The early time variations appear to be in good agreement with the Pg statistics presented earlier and can account for both the dominantly double peaked, as well as the single peaked, $H$ component variations seen on the ground. However, as the wave evolves and the additional toroidal component is driven, the disturbance becomes increasingly elliptically polarised and asymptotes towards a purely linear toroidal oscillation [see *Mann and Wright*, 1995, Figure 5]. This asymptotic toroidal state does not appear to occur in the EISCAT magnetometer cross data that we presented earlier. However, this can be explained by considering the timescales over which the driving mechanism and ionospheric dissipation act. The magnetospheric fields which result when a wave is con-

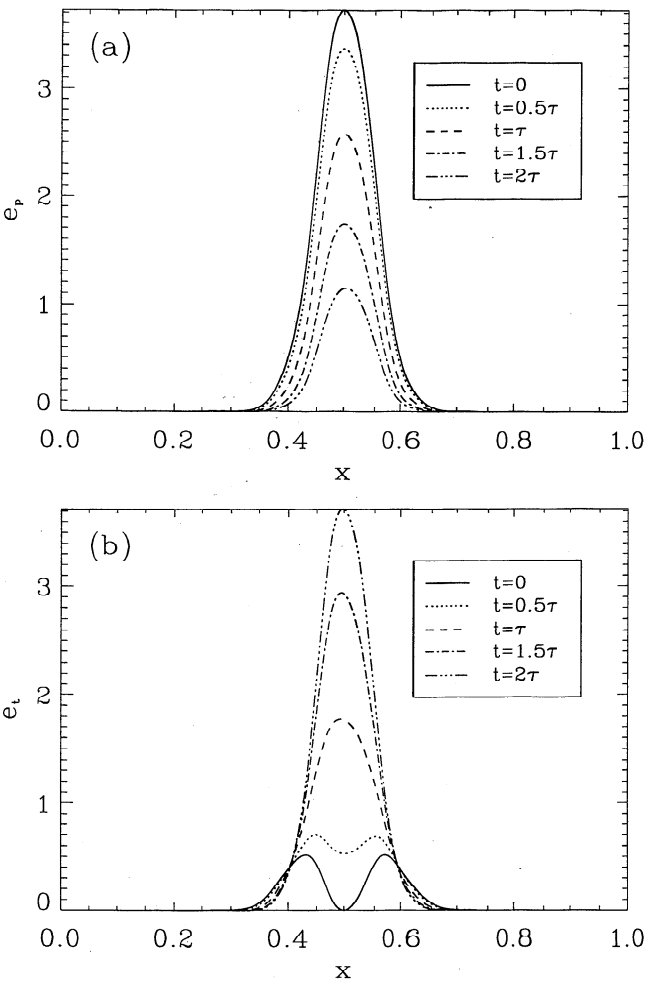


**Figure 8.** The Pg (a) poloidal and (b) toroidal energy densities $e_p$ and $e_t$ as a function of $\hat{\mathbf{x}}$ at $t = 0$ (solid line) and multiples of $\tau$ (dashed lines).

tinually driven can be envisaged as a continual summation of ionospherically decaying solutions to the undriven initial value problem considered here. Consequently, it may be possible for the waves to develop an overall structure in which only part of the asymptotic evolution has occurred, and we discuss this in the next section.

## 6. Discussion

The main discrepancy between our modeling and the Pg observations is the extent to which the polarization evolution from guided poloidal to toroidal occurs. The most significant simplification assumed in our model is that of infinite ionospheric conductivity. Pg waves are usually observed predawn where the height-integrated Pedersen conductivity $\Sigma_P$ is typically much lower than average dayside values. Assuming $\Sigma_P \sim 0.5 - 1$ mhos (compared to typical dayside values of $\sim 10 - 20$ mhos) and using the numerical results of *Newton et al.* [1978], we find second harmonic guided poloidal waves have damping decrements $\gamma/\omega \sim 0.075 - 0.04$, corresponding to e-fold decay times $\tau_I \sim 2 - 4$ wave periods. Since the damping of second harmonic toroidal waves is of a similar magnitude, we would expect waves to only display the polarization evolution discussed earlier if it occurs on a timescale $\lesssim \tau_I$.

Assuming a dipole magnetic field geometry, a density profile $\rho \sim \rho_0 r^{-p}$ with $p = 3$, and estimating equatorial mass densities from those deduced by *Poulter et al.* [1984], we used the results of *Cummings et al.* [1969] and *Orr and Matthew* [1971] to estimate $d\omega_A/dx \approx 2.8 \times 10^{-9}$ rads s$^{-1}$m$^{-1}$ for a 100 s second harmonic guided poloidal wave at L = 6.5. Assuming that typically $m \sim 30$ and 100 for Pgs and afternoon poloidal Alfvén waves respectively, we estimate poloidal lifetimes of 2.6 and 8.5 periods respectively. For Pg waves near dawn we find $\tau_I \sim \tau$ and hence we would only expect a small wave evolution before the signals are damped by the ionosphere. Consequently, for a continually driven pulsation, the observed fields will be dominated by the amplitude profiles of the initial oscillations. Exactly at resonance, where there is initially a toroidal node, we would expect only a small amplitude toroidal component to develop so that the double peaked toroidal amplitude variation would be maintained. This is in good agreement with the Pg amplitude statistics.

In the afternoon sector, where poloidal Alfvén waves are often observed in space, $\Sigma_P$ will have more typical dayside values. Again, using the results of *Newton et al.*, [1978], and assuming $\Sigma_P \sim 10$ mhos, gives $\gamma/\omega \sim 0.004$ and hence $\tau_I \sim 40$ periods. Neglecting any variation in Alfvén speed with local time, we conclude that poloidal Alfvén waves with $m \sim 100$ will have $\tau = 8.5$ periods, and hence $\tau_I > \tau$ in this case. Consequently, bounce resonance driven waves in the afternoon could experience significant evolution from guided poloidal to toroidal before they are heavily damped by the ionosphere, and once they are no longer being driven may approach an asymptotic toroidal polarization state.

The differences in the azimuthal wave numbers of Pgs and poloidal Alfvén waves can also explain why Pgs are observed from the ground and poloidal Alfvén waves are not. Ground-based Pg observations have been characterized by moderately large azimuthal wave numbers, with typical values of $m \sim 20 - 40$ [*Rostoker et al.*, 1979; *Glassmeier*, 1980; *Hillebrand et al.*, 1982; *Poulter et al.*, 1983; *Chisham et al.*, 1990; *Takahashi et al.*, 1992], where the waves are assumed to vary as $\exp(im\phi)$ and $\phi$ is a the azimuthal coordinate. *Hughes and Southwood* [1976] concluded that Alfvén waves in space have magnetic signals which decay to the ground according to $\exp(-k_\perp h)$, where $k_\perp$ is the perpendicular wave number and $h$ is the height of the ionospheric $E$ region. If we assume that both Pgs and poloidal Alfvén waves have similar radial magnetospheric widths ($\sim 1\ R_E$) and have azimuthal wave numbers $\sim 30$ and 100, respectively, then the Pg amplitude would decay to ~7% of its ionospheric value whereas that of the poloidal Alfvén wave would decay to ~1% of its ionospheric value. Phase mixing of the poloidal Alfvén waves due to their longer ionospheric lifetimes ($\tau_I \sim 40$ periods) increases $k_\perp$ and causes further decay. This would explain why Pgs can be observed from the ground, while poloidal Alfvén waves with larger azimuthal wave numbers, despite being observed in the magnetosphere, appear to have no conjugate ground magnetometer signal.

If the waves evolve in the way described earlier, the additional toroidal component they generate should be in quadrature with the initial toroidal signal. For waves with azimuthally standing structure (as well as standing along the background field), such as those presented in section 5, $\xi_x^P$ is of the form

$$\begin{aligned} \xi_x^P &= \mathrm{Re}\{H \cos\omega_A(x)t \exp i\lambda y \sin k_z z\} \\ &= H \cos\omega_A(x)t \cos\lambda y \sin k_z z \end{aligned} \quad (12)$$

where $H$ is the amplitude of the poloidal disturbance, and from (5),

$$\begin{aligned} \xi_y^P &= \left[\frac{H\omega_A'(x)t}{\lambda} \sin\omega_A(x)t \right. \\ &\quad \left. - \frac{H'}{\lambda} \cos\omega_A(x)t\right] \sin\lambda y \sin k_z z \\ &= -I \cos(\omega_A(x)t + \phi) \sin\lambda y \sin k_z z \end{aligned} \quad (13)$$

where $I = (H^2\omega_A'(x)^2t^2 + H'^2)^{\frac{1}{2}}/\lambda$ and $\phi = \tan^{-1}(H\omega_A'(x)t/H')$, and where a prime denotes $d/dx$ (note that conservation of total energy means that the amplitude of the poloidal disturbance $H$ will decrease in time; see *Mann et al.* [1997] for more details). In this case the waves initially oscillate in phase, and for waves in the plasmatrough where the Alfvén frequencies decrease with radial distance (i.e., $\omega_A'(x)$ is negative) and if $\lambda$ is negative, the component resulting from the wave

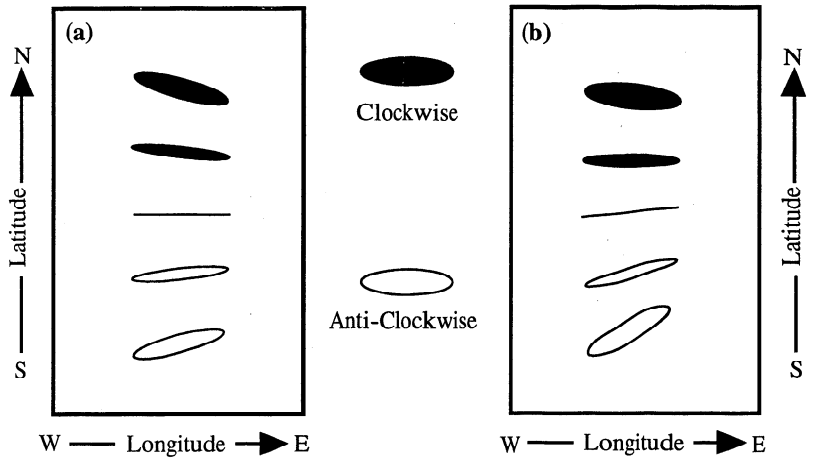


**Figure 9.** Schematic diagram of the ground orientation of the polarization ellipses of Pg waves with azimuthally propagating phase. (a) Possible polarizations of Pgs driven by drift bounce resonance. (b) The modification of these polarizations after the partial wave evolution from guided poloidal to toroidal.

evolution would have the effect of adding a clockwise polarized component to the wave signal (as observed in the direction of the geomagnetic field line). This would shift the ground-based observation of the position of linear polarization equatorward of the position of the east-west oriented polarization ellipse.

For azimuthally traveling waves (e.g., waves driven by the drift bounce resonance mechanism), $\xi_x^P$ is of the form

$$\begin{aligned} \xi_x^P &= \mathrm{Re}\{H \exp(-i\omega_A(x)t) \exp i\lambda y \sin k_z z\} \\ &= H \cos(\omega_A(x)t - \lambda y) \sin k_z z. \end{aligned} \quad (14)$$

and (5) generates the associated toroidal signal

$$\begin{aligned} \xi_y^P &= \left[\frac{H\omega_A'(x)t}{\lambda} \cos(\omega_A(x)t - \lambda y) \right. \\ &\quad \left. + \frac{H'}{\lambda} \sin(\omega_A(x)t - \lambda y)\right] \sin k_z z \\ &= I \sin(\omega_A(x)t - \lambda y + \phi) \sin k_z z. \end{aligned} \quad (15)$$

In this case the initial (traveling) $\xi_x^P$ and $\xi_y^P$ are in quadrature. For waves in the plasmatrough with negative $\lambda$ (westward phase propagation), they are polarized clockwise (viewed in the direction of the geomagnetic field line) poleward and anticlockwise equatorward of linear polarization (in good agreement with Figure 5). Moreover, the driven toroidal component is in phase with the initial poloidal component and rotates the polarization azimuths so that the ground-based observation of the position of linear polarization is again equatorward of the position of the east-west oriented ellipse. If the undriven wave solutions evolve on the same timescale as the ionospheric damping, only a small evolution would occur which would only shift the position of linear polarization slightly equatorward of the position of the east-west oriented ellipse. We schematically illustrate in Figure 9 how this shift might effect the latitudinal polarization variation of Pgs with azimuthally propagating phase fronts. This agrees with the statistical variation shown in Figure 5, and suggests that the polarization evolution is occuring to a small extent with Pgs.

Pg waves are observed predawn, with wave trains $\sim$ 30 cycles long. However, we have already estimated an undriven lifetime of only a few eigenperiods due to ionospheric damping. This appears to be good evidence that Pgs are being continually driven. More evidence that the waves are being continually driven comes from the observations of *Chisham et al.* [1992]. They calculated that the apparent azimuthal propagation speed of the leading wavefront of the Pg disturbance propagated westward faster than the magnetometer field of view corotated eastward with the Earth (i.e., the actual azimuthal propagation direction of the wave was westward). The actual propagation speed (after removal of the effect of the Earth's rotation) equated well with the drift velocity of $\sim 10 - 20$ keV protons. A possible Pg driving mechanism is drift bounce resonance with energetic protons [*Southwood et al.*, 1969; *Southwood*, 1976], and protons with energies $\sim 10 - 20$ keV could drive second harmonic waves having periods and azimuthal wavenumbers typical of Pgs.

If Pgs are associated with westward drifting protons with energies $\sim 10 - 20$ keV which maintain a constant phase relation with the azimuthal phase fronts of the wave, then the phase velocity of the waves should equal the drift velocity of the protons. *Glassmeier* [1980] suggested that the Pg polarization variation that he observed could be explained by field aligned current elements which were drifting westwards. On the basis of an observed drift velocity of $\sim$ 8 km $s^{-1}$ in the ionosphere he concluded that since his event lasted for $\sim$ 30 periods, it should exist for $\sim$ 300° in azimuth. This was in contrast to the observed localiza-

tion of the disturbance. However, our suggestion that Pgs are guided poloidal Alfvén waves with westward phase propagation can resolve this apparent contradiction. Field-aligned currents are generated by poloidal Alfvén waves. Poloidal Alfvén waves with a westward phase propagation would produce current elements of the type observed by *Glassmeier* [1980]. However, they would not have a westwards group velocity (they are Alfvénic and hence have no group velocity perpendicular to the background field). Consequently, if Pgs are poloidal Alfvén waves which are being continually driven by drift bounce resonance with protons, they can have wave trains which oscillate for many cycles and show westward phase propagation, while still being localized in space. Moreover, if the bounce resonance mechanism drives a disturbance having a spatial extent greater than half an azimuthal wavelength, then a meridional separator line of the type seen by *Glassmeier* [1980] could exist, in addition to the latitudinal demarcation line seen in the Pg statistics presented here and in other Pg observational data [*Hillebrand*, 1976; *Glassmeier*, 1980; *Hillebrand et al.*, 1982; *Chisham et al.*, 1990]

## 7. Summary

We have presented the results of a statistical analysis of the latitudinal variation of 34 Pg events observed by the EISCAT magnetometer cross. The statistics show that Pgs are exclusively polarized in a clockwise sense poleward, and an anticlockwise sense equatorward, of the latitudinal position of linear polarization. Despite being polarized northeast to southwest equatorward, and northwest to southeast poleward of linear polarization, the polarization azimuth is oriented east-west at a location poleward of linear polarization. The amplitude statistics show that the latitudinal variation of the $D$ component has a distinct peak characteristic of a resonance, whilst the $H$ component has a tendency to show a double peaked variation, often having a dip at the position of the maximum $D$ component amplitude.

By employing an MHD numerical code to model Pg-like disturbances, we considered the time dependent evolution of guided poloidal Alfvén waves in an inhomogeneous box model magnetosphere. On the basis of the statistical and numerical results, we have suggested the following model for Pg wave evolution. Energetic protons ($\sim 10 - 20$ keV) drift westward from a nightside injection region into the morning sector. On $L$ shells unstable to wave excitation, the drift bounce resonance mechanism drives dominantly guided poloidal Alfvén waves with westward phase propagation. Waves with Pg-like characteristics which occur predawn have undriven lifetimes of only a few wave periods due to ionospheric damping, and hence Pgs must be being continually driven. They experience a polarization evolution from guided poloidal to toroidal over a similar (or longer) timescale to that of the ionospheric damping (i.e., they have ideal poloidal lifetimes $\gtrsim \tau_I$) and hence only partially evolve toward a purely toroidal polarization. This model can successfully explain both the Pg amplitude and polarization statistics which we have presented.

In the afternoon sector, poloidal Alfvén waves similar to Pgs are observed, but these generally have larger azimuthal wave numbers. In the afternoon, ionospheric damping should typically occur on a timescale longer than the ideal poloidal lifetime, and hence we would expect afternoon poloidal Alfvén waves to typically display a greater evolution towards a purely toroidal polarization state than the Pgs we have studied here. This is difficult to verify using ground based data as these waves are screened by the ionosphere due to their larger azimuthal wave number ($m \sim 100$ for typical poloidal Alfvén waves). More detailed observations in space might allow this theory to be tested.

**Acknowledgments.** We are extremely grateful to Hermann Lühr for supplying the EISCAT magnetometer cross data. The EISCAT magnetometer cross is a joint enterprise of the Finnish Meteorological Institute, the Sodankyla Geophysical Observatory, and the Technical University Braunschweig. The authors would also like to thank Andrew Wright for useful discussions and comments on the manuscript. This work was supported by the U.K. Particle Physics and Astronomy Research Council grants GR/J88388 and GR/K94133.

The Editor thanks Kazue Takahashi and another referee for their assistance in evaluating this paper.

## References

Beamish, D., H. W. Hanson, and D. C. Webb, Complex demodulation applied to Pi2 geomagnetic pulsations, *Geophys. J. R. Astron. Soc.*, *58*, 471, 1979.

Boyd, T. J. N., and J. J. Sanderson, *Plasma Dynamics*, Nelson, London, 1969.

Brekke, A., T. Feder, and S. Berger, Pc4 giant pulsations recorded in Tromso, 1929-1985, *J. Atmos. Terr. Phys.*, *49*, 1027, 1987.

Cao, M., R. L. McPherron, and C. T. Russell, Statistical study of ULF wave occurrence in the dayside magnetosphere, *J. Geophys. Res.*, *99*, 8731, 1994.

Chisham, G., and D. Orr, Statistical studies of giant pulsations (Pgs): Harmonic mode, *Planet. Space Sci.*, *39*, 999, 1991.

Chisham, G., and D. Orr, The association between giant pulsations (Pgs) and the auroral oval, *Ann. Geophys.*, *12*, 649, 1994.

Chisham, G., D. Orr, M. J. Taylor, and H. Lühr, The magnetic and optical signature of a Pg pulsation, *Planet. Space Sci.*, *38*, 1443, 1990.

Chisham, G., D. Orr, and T. K. Yeoman, Observations of a giant pulsation (Pg) across an extended array of ground magnetometers and on auroral radar, *Planet. Space Sci.*, *40*, 953, 1992.

Chisham, G., D. Orr, T. K. Yeoman, D. K. Milling, M. Lester, and J. A. Davies, The polarization of Pc5 ULF waves around dawn: A possible ionospheric conductivity gradient effect, *Ann. Geophys.*, *13*, 159, 1995.

Cummings, W. D., R. J. O'Sullivan, and P. J. Coleman Jr., Standing Alfvén waves in the magnetosphere, *J. Geophys. Res.*, *74*, 778, 1969.

Dungey, J. W., Hydromagnetic waves, in *Physics of Geomagnetic Phenomena*, vol. 2, edited by S. Matsushita and W. H. Campbell, p. 913, Academic, San Diego, Calif., 1967.

Glassmeier, K.-H., Magnetometer array observations of a giant pulsation event, *J. Geophys.*, *48*, 127, 1980.

Glassmeier, K.-H., On the influence of ionospheres with non-uniform conductivity distributions on hydromagnetic waves, *J. Geophys.*, *54*, 125, 1984.

Green, C. A., Observations of Pg pulsations in the northern auroral zone and at other lower latitude conjugate regions, *Planct. Space Sci.*, *27*, 63, 1979.

Green, C. A., Giant pulsations in the plasmasphere, *Planet. Space Sci.*, *33*, 1155, 1985.

Hillebrand, O., Spatial characteristics of giant pulsations, *J. Geophys.*, *42*, 257, 1976.

Hillebrand, O., J. Munch, and R. L. McPherron, Ground-satellite correlative study of a giant pulsation event, *J. Geophys.*, *51*, 129, 1982.

Hughes, W. J., and D. J. Southwood, The screening of micropulsation signals by the atmosphere and ionosphere, *J. Geophys. Res.*, *81*, 3234, 1976.

Kokubun, S., K. N. Erickson, T. A. Fritz, and R. L. McPherron, Local time asymmetry of Pc4-5 pulsations and associated particle modulations at synchronous orbit, *J. Geophys. Res.*, *94*, 6607, 1989.

Lühr, H., S. Thurey, and N. Klocker, The Eiscat-Magnetometer cross, *Geophys. Surv.*, *6*, 305, 1984.

Mann, I. R., and A. N. Wright, Finite Lifetimes of Ideal Poloidal Alfvén waves, *J. Geophys. Res.*, *100*, 23,677, 1995.

Mann, I. R., A. N. Wright, and P. S. Cally, Coupling of magnetospheric cavity modes to field line resonances: A study of resonance widths, *J. Geophys. Res.*, *100*, 19,441, 1995.

Mann, I. R., A. N. Wright, and A. W. Hood, Multiple-timescales analysis of ideal poloidal Alfvén waves, *J. Geophys. Res.*, *102*, 2381, 1997.

Newton, R. S., D. J. Southwood, and W. J. Hughes, Damping of geomagnetic pulsations by the ionosphere, *Planet. Space Sci.*, *26*, 201, 1978.

Orr, D., and J. A. D. Matthew, The variation of geomagnetic micropulsation periods with latitude and the plasmapause, *Planet. Space Sci.*, *19*, 897, 1971.

Poulter, E. M., and W. Allan, Transient ULF pulsation decay rates observed by ground magnetometers: the contribution of spatial integration, *Planet. Space Sci.*, *33*, 607, 1985.

Poulter, E. M., W. Allan, E. Nielsen, and K.-H. Glassmeier, STARE radar observations of a Pg pulsation. *J. Geophys. Res.*, *88*, 5668, 1983.

Poulter, E. M., W. Allan, J. G. Keys, and E. Nielsen, Plasmatrough ion mass densities determined from ULF pulsation eigenperiods, *Planet. Space Sci.*, *32*, 1069, 1984.

Radoski, H. R., Highly asymmetric MHD resonances: The guided poloidal mode, *J. Geophys. Res.*, *72*, 4026, 1967.

Rostoker, G, H.-L. Lam, and J. V. Olson, Pc4 giant pulsations in the morning sector, *J. Geophys. Res.*, *84*, 5153, 1979.

Southwood, D. J., Some features of field line resonances in the magnetosphere, *Planet. Space Sci.*, *22*, 483, 1974.

Southwood, D. J., A general approach to low-frequency instability in the ring current plasma, *J. Geophys. Res.*, *81*, 3340, 1976.

Southwood, D. J., Low frequency pulsation generation by energetic particles, *J. Geomagn. Geoelectr.*, *32*, SII 75, 1980.

Southwood, D. J., J. W. Dungey, and R. J. Etherington, Bounce resonant interaction between pulsations and trapped particles, *Planet. Space Sci.*, *17*, 349, 1969.

Takahashi, K., N. Sato, J. Warnecke, H. Lühr, H. E. Spence, and Y. Tonegawa, On the standing wave mode of giant pulsations, *J. Geophys. Res.*, *97*, 10,717, 1992.

Taylor, M. J., G. Chisham, and D. Orr, Pulsating auroral forms and their association with geomagnetic giant pulsations, *Planet. Space Sci.*, *37*, 1477, 1989.

---

Gareth Chisham, Ian R. Mann, Astronomy Unit, Queen Mary and Westfield College, Mile End Road, London E1 4NS, UK (e-mail: G.Chisham@qmw.ac.uk; I.Mann@qmw.ac.uk)

David Orr, Department of Physics, University of York, Heslington, York YO1 5DD, UK

(Received May 13, 1996; revised September 19, 1996; accepted January 24, 1997.)